Progress In Electromagnetics Research, PIER 74, 113–130, 2007

A STABLE INTEGRAL EQUATION SOLVER FOR ELECTROMAGNETIC SCATTERING BY LARGE SCATTERERS WITH CONCAVE SURFACE

M. S. Tong

Department of Electrical and Computer Engineering
University of Illinois at Urbana-Champaign
1406 West Green Street
Urbana, IL 61820, USA

Abstract—Electromagnetic scattering by electrically large scatterers usually requires a large number of unknowns. To reduce the matrix size, one expects to choose a small sampling rate for the unknown function. In the method of moments (MoM) scheme, this rate is about 10 unknowns per wavelength for electrically small or medium scatterers. However, this rate may not work well for electrically large scatterers with a concave surface. The concave area on the scatter is observed to be the oscillatory part in the solution domain. The oscillation property requires more samplings to eliminate the numerical noises. The multiscalets with a multiplicity of two are higher-order bases. It is shown that the multiscalets are more suitable to represent the unknown function with oscillatory characteristic. Furthermore, the testing scheme under the discrete Sobolev-type inner product allows the MoM have the derivative sampling which enhances the tracking quality of the multiscalets further. Numerical Examples of scattering by 1000 and 1024 wavelength 2D scatterers demonstrate that the use of multiscalets in the MoM can keep the same discretization size for electrically large scatterers as for electrically small scatterers without losing the accuracy of the solution. In contrast, the traditional MoM and Nyström method require the finer discretization scheme if achieving a stable solution.

1. INTRODUCTION

Method of moments (MoM) is one of the most widely used numerical methods in solving electromagnetic (EM) integral equations for EM scattering problems [1–3]. In the MoM scheme, it is commonly recognized that the discretization for an electrically small or medium geometry is about ten unknowns per wavelength if the general basis functions such as pulse and triangular shape functions are used. However, when the electrical size of a scatter increases due to the increase of the operating frequency and reaches a very large size, say 1000 wavelengths, the numerical solution may not be good enough. There exist big numerical noises in the convex area and unsmooth oscillations can be seen in the concave area in the solution domain. For such scattering problem, the conventional MoM may not provide an acceptable solution if still using the usual discretization scheme and finer meshes are usually needed.

Fast Multiple Method (FMM) is thought of as a very robust numerical approach in dealing with electrically large problems [4–9]. The FMM can solve a matrix equation with 20 million unknowns on a common workstation [7]. However, the FMM is based on the system matrix produced by the MoM, which implies that the FMM is a matrix solver instead of matrix producer. If the resulting MoM matrix cannot represent the original problem in a good approximation due to the insufficient sampling on the unknown function, the FMM may not yield a good solution. Furthermore, the FMM is not easy to implement although it can greatly save memory usage and CPU time.

Nyström method is also a potential numerical scheme to solve electrically large problems [8–10]. Unlike the MoM, the Nyström method applies a numerical quadrature rule to discretized integral equations directly if the integral kernels are smooth. The values of the unknown function at the corresponding quadrature points are selected as the unknowns to be solved. Therefore, most of matrix entries can be produced in an easier and more direct style and the matrix filling time is dramatically reduced. If the integral kernels are singular, a local correction scheme is needed to generate corresponding diagonal matrix entries [10]. This will prevent the method from being used sometimes. Also, Nyström method requires a larger number of unknowns than MoM because the unknowns are defined on each of quadrature points and there are multiple points on each meshed element.

Wavelet based algorithms have been developed and widely used in solving EM problems recently [13–17]. If the multiscalets are used as basis functions and the testing procedure defined in the Sobolev space is implemented in the MoM, the hybrid algorithm, multiscalet based

moment method (MBMM), exhibits a very attractive performance [14, 15]. These attractive qualities come from the higher-order property of the multiscalets with a multiplicity of two and the derivative tracking for the unknown functions. The resulting algorithm is specially suitable for solving electrically large problems because it can be used in the same way as in the small problems without increasing the density of discretization and other complexity. The numerical solution is continuously stable from the small-size scatter to the large-size scatter, differing from the conventional MoM.

In the following sections, we briefly introduce the MBMM and the implementation for 2D scattering problems. As a comparison, we also present the implementing formulations of Nyström method. Two numerical examples are used to illustrate the difference between the MBMM, the conventional MoM and Nyström method.

2. MULTISCALETS AND MBMM

Multiscalets are the matrix-vector version of the regular scalets. If the regular scalet is defined as

$$\phi(t) = \sum_k h_k \phi(2t - k) \tag{1}$$

where h_k is the lowpass filter coefficient, the corresponding multiscalet is then defined as

$$|\phi(t)\rangle = \sum_k C_k |\phi(2t - k)\rangle \tag{2}$$

where $C_k = [C_k]_{r\times r}$ is the lowpass coefficient matrix of $r \times r$, $|\phi(t)\rangle = [\phi_o(t), \phi_1(t), \cdots, \phi_{r-1}(t)]^T$ is the multiscalet vector of $r \times 1$, and r is the multiplicity. In the above matrix-vector dilation equation, the only nonzero lowpass coefficients are C_0, C_1, and C_2, leading to a compact support $[0, 2]$ for $|\phi(t)\rangle$. The multiscalet can be easily derived either by numerical iteration or by the analytical approach. For $r = 2$, the derived explicit form of the multiscalet is

$$\begin{aligned} \phi_0(t) &= \begin{cases} 3t^2 - 2t^3 & t \in [0, 1] \\ 3(2-t)^2 - 2(2-t)^3 & t \in [1, 2] \end{cases} \\ \phi_1(t) &= \begin{cases} t^3 - t^2 & t \in [0, 1] \\ -(2-t)^3 + (2-t)^2 & t \in [1, 2]. \end{cases} \end{aligned} \tag{3}$$

The multiscalets satisfy the Sobolev orthogonality at the zeroth scaling level which is defined in a discrete Sobolev inner product space. The

Sobolev orthogonality of the multiscalets implies

$$\begin{aligned}\langle \phi_i(t-m), \phi_k(t-n)\rangle &= \sum_{j=0}^{r-1}\sum_{p\in Z} \phi_i^{(j)}(p-m)\phi_k^{(j)}(p-n) \\ &= \sum_{j=0}^{r-1} \phi_i^{(j)}(1-m)\phi_k^{(j)}(1-n) \\ &= \sum_{j=0}^{r-1} \delta_{i,j}\delta_{k,j}\delta_{m,n} \\ &= \delta_{i,k}\delta_{m,n}. \end{aligned} \tag{4}$$

The use of the above nature of the multiscalets yields the multiscalet based moment method (MBMM) [14], which enforces the derivative sampling and tracking for the integral equations in addition to the point-matching procedure. In the MBMM, the unknown function is expanded using the multiscalet basis functions defined on the contour of a scatterer

$$J(\tau') = \sum_{n=1}^{N} [D_n^f \phi_{0n}(\tau') + D_n^d \phi_{1n}(\tau')] \tag{5}$$

where D_n^f and D_n^d are the expansion coefficients and the superscripts f and d denote the function sampling and derivative sampling respectively. Note that we have split the scatterer into N segments with a length of h and τ_n' $(n = 1, 2, \cdots N+1)$ are the corresponding nodes. The multiscalets are then taking the following form after being shifted and scaled to fit the segments

$$\begin{aligned}\phi_{0n}(t') &= \begin{cases} 3t'^2 - 2t'^3 & \tau_{n-1}' \le \tau' \le \tau_n' \\ 3(2-t')^2 - 2(2-t')^3 & \tau_n' \le \tau' \le \tau_{n+1}' \end{cases} \\ \phi_{1n}(t') &= \begin{cases} t'^3 - t'^2 & \tau_{n-1}' \le \tau' \le \tau_n' \\ -(2-t')^3 + (2-t')^2 & \tau_n' \le \tau' \le \tau_{n+1}'. \end{cases} \end{aligned} \tag{6}$$

where $t' = (\tau' - \tau_{n-1}')/h$ and τ' is the arc length along the contour measured from a reference point. Testing the discretized integral equation using the multiscalet weighting functions and making use of the Sobolev orthogonality of the multiscalets in (4), we can write that

$$F^{inc}(\tau_m) = \sum_{n=1}^{N+1} g_{0n}(\tau_m) D_n^f + \sum_{n=1}^{N+1} g_{1n}(\tau_m) D_n^d$$

$$F'^{inc}(\tau_m) = \sum_{n=1}^{N+1} g'_{0n}(\tau_m) D_n^f + \sum_{n=1}^{N+1} g'_{1n}(\tau_m) D_n^d \qquad m = 1, 2, \cdots, N+1 \tag{7}$$

where F^{inc} is the known incident field in the scattering problems and g_{pn} $(p = 0, 1)$ are the matrix elements evaluated by integrating the Green's function and multiscalet bases within a segment. The resulting matrix equation is solved using the standard numerical methods and $J(\tau')$ is then found from (5).

3. MBMM FORMULATIONS FOR EM SCATTERING

Consider the TM^z wave scattering by a 2D conducting scatterer which can be represented by the electric field integral equation (EFIE) [18]

$$E_z^i(\boldsymbol{\rho}) = \frac{\kappa\eta}{4} \int_C J_z(\boldsymbol{\rho}') H_0^{(2)}(\kappa|\boldsymbol{\rho} - \boldsymbol{\rho}'|) d\ell' \quad \boldsymbol{\rho} \text{ and } \boldsymbol{\rho}' \text{ on } C. \tag{8}$$

where E_z^i denotes the incident electric field, J_z denotes the unknown current density on the contour C of the scatterer and $H_0^{(2)}$ denotes the zeroth-order second kind of Hankel function. To determine the current density J_z, we first discretize the contour of the scatterer into N segments with a step size of h. We then expand J_z using the multiscalet bases as shown in (3), and test the integral equations in terms of the discrete Sobolev inner product. This leads to the following MBMM system equations

$$\begin{aligned} E_z^{inc}(x_0^m, y_0^m) &= \sum_{n=1}^{N} D_n^f \left\{ \int_{-h}^{0} (3t'^2 - 2t'^3) H_0^{(2)}(\kappa s_1^{mn}) d\tau' \right. \\ &+ \left. \int_0^h [3(2-t')^2 - 2(2-t')^3] H_0^{(2)}(\kappa s_2^{mn}) d\tau' \right\} \\ &+ \sum_{n=1}^{N} D_n^d \left\{ \int_{-h}^{0} (t'^3 - t'^2) H_0^{(2)}(\kappa s_1^{mn}) d\tau' \right. \\ &+ \left. \int_0^h [-(2-t')^3 + (2-t')^2] H_0^{(2)}(\kappa s_2^{mn}) d\tau' \right\} \end{aligned}$$

$$\frac{dE_z^{inc}(x_0^m, y_0^m)}{d\tau} = \sum_{n=1}^{N} D_n^f \left\{ \int_{-h}^{0} (3t'^2 - 2t'^3) V_1 d\tau' \right.$$

$$
\begin{aligned}
&+ \quad \int_0^h [3(2-t')^2 - 2(2-t')^3] V_2 d\tau' \Bigg\} \\
&+ \quad \sum_{n=1}^{N} D_n^d \Bigg\{ \int_{-h}^{0} (t'^3 - t'^2) V_1 d\tau' \\
&+ \quad \int_0^h [-(2-t')^3 + (2-t')^2] V_2 d\tau' \Bigg\} \\
&\qquad m = 1, 2, \cdots, N
\end{aligned} \tag{9}
$$

where

$$
\begin{aligned}
t' &= 1 + \frac{\tau'}{h} \\
V_1 &= \frac{\kappa H_0^{(2)'}(\beta s_1^{mn})}{s_1^{mn}} \cdot [(x_0^m - x_1^{'n})(\cos\alpha_{1m} + \cos\alpha_{2m}) \\
&+ (y_0^m - y_1^{'n})(\sin\alpha_{1m} + \sin\alpha_{2m})] \\
V_2 &= \frac{\kappa H_0^{(2)'}(\beta s_2^{mn})}{s_2^{mn}} \cdot [(x_0^m - x_2^{'n})(\cos\alpha_{1m} + \cos\alpha_{2m}) \\
&+ (y_0^m - y_2^{'n})(\sin\alpha_{1m} + \sin\alpha_{2m})] \\
s_1^{mn} &= \sqrt{(x_0^m - x_1^{'n})^2 + (y_0^m - y_1^{'n})^2} \\
s_2^{mn} &= \sqrt{(x_0^m - x_2^{'n})^2 + (y_0^m - y_2^{'n})^2}.
\end{aligned} \tag{10}
$$

In the above formulations, τ is the arc length measured from the mth node (x_0^m, y_0^m), and (x_1^m, y_1^m) and (x_2^m, y_2^m) are the observation position variables in the two neighboring segments of the node. They are related to each other by

$$
\begin{aligned}
&\begin{cases} x_1^m = x_0^m + \tau\cos\alpha_{1m} \\ y_1^m = y_0^m + \tau\sin\alpha_{1m} \end{cases} \\
&\qquad\qquad -h \le \tau \le 0 \\
&\begin{cases} x_2^m = x_0^m + \tau\cos\alpha_{2m} \\ y_2^m = y_0^m + \tau\sin\alpha_{2m} \end{cases} \\
&\qquad\qquad 0 \le \tau \le h.
\end{aligned} \tag{11}
$$

Similarly, $(x_1^{'n}, y_1^{'n})$ and $(x_2^{'n}, y_2^{'n})$ are the source position variables in the two neighboring segments of the nth node (x_0^n, y_0^n) and they are

related as

$$\begin{cases} x_1'^n = x_0^n + \tau' \cos\alpha_{1n} \\ y_1'^n = y_0^n + \tau' \sin\alpha_{1n} \end{cases} \quad -h \le \tau' \le 0$$

$$\begin{cases} x_2'^n = x_0^n + \tau' \cos\alpha_{2n} \\ y_2'^n = y_0^n + \tau' \sin\alpha_{2n} \end{cases} \quad 0 \le \tau' \le h. \tag{12}$$

Figure 1 illustrates the above coordinate relationship between a node and a point on its neighboring segments on a contour C for a scatterer. In this figure, (x_0^n, y_0^n) is the coordinate of the nth node, α_{1n} and α_{2n} are the directional angles of the two neighboring segments connecting to the node, and τ' is the distance between a source point on the neighboring segment and the node. If n is replaced by m and τ' is replaced by τ, the same relationship is valid for the observation position variables.

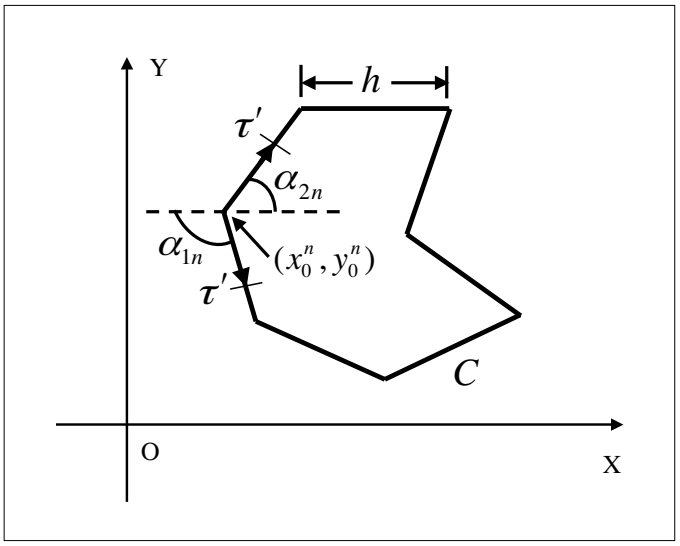

Figure 1. Coordinate relationship for a node and its neighboring segments on a contour C.

As a comparison, we also derive the corresponding MoM system equation with the triangle bases

$$\begin{aligned}
&\int_{-h}^{0}\left(1+\frac{\tau}{h}\right)E_z^{inc}(x_1^m,y_1^m)d\tau+\int_{0}^{h}\left(1-\frac{\tau}{h}\right)E_z^{inc}(x_2^m,y_2^m)d\tau\\
&=\sum_{n=1}^{N}C_n\left[\int_{-h}^{0}\left(1+\frac{\tau}{h}\right)d\tau\int_{-h}^{0}\left(1+\frac{\tau'}{h}\right)H_0^{(2)}(\kappa d_{11})d\tau'\right.\\
&+\int_{-h}^{0}\left(1+\frac{\tau}{h}\right)d\tau\int_{0}^{h}\left(1-\frac{\tau'}{h}\right)H_0^{(2)}(\kappa d_{12})d\tau'\\
&+\int_{0}^{h}\left(1-\frac{\tau}{h}\right)d\tau\int_{-h}^{0}\left(1+\frac{\tau'}{h}\right)H_0^{(2)}(\kappa d_{21})d\tau'\\
&\left.+\int_{0}^{h}\left(1-\frac{\tau}{h}\right)d\tau\int_{0}^{h}\left(1-\frac{\tau'}{h}\right)H_o^{(2)}(\kappa d_{22})d\tau'\right]\\
&m=1,2,\cdots,N. \qquad (13)
\end{aligned}$$

where $d_{ij}=\sqrt{(x_i^m-x_j'^n)^2+(y_i^m-y_j'^n)^2}$ with $i=1,2$ and $j=1,2$. These system equations can be easily solved with the desired expansion coefficients using the iteration methods such as Biconjugate Gradient Stabilized Method (BCGSTAB) or Generalized Minimal Residual Method (GMRES) with a moderate memory usage if the system matrix is very large [19].

4. NYSTRÖM METHOD

For the EFIE represented by (8), the Nyström method is implemented as follows. By the discretization with N segments, the EFIE becomes

$$E_z^i(\boldsymbol{\rho})=\sum_{i=1}^{N}\int_{\Delta C}g(\boldsymbol{\rho},\boldsymbol{\rho}')J_z(\boldsymbol{\rho}')d\ell' \quad \boldsymbol{\rho} \text{ and } \boldsymbol{\rho}' \text{ on } C \qquad (14)$$

where $g(\boldsymbol{\rho},\boldsymbol{\rho}')=\frac{\kappa\eta}{4}H_0^{(2)}(\kappa|\boldsymbol{\rho}-\boldsymbol{\rho}'|)$. In each segment, the integration can be replaced by the summation using an appropriate quadrature rule, say Gaussian-Legendre quadrature. We then obtain

$$E_z^i(\boldsymbol{\rho})=\sum_{i=1}^{N}\sum_{j=1}^{P}g(\boldsymbol{\rho},\boldsymbol{\rho}'_{ij})J_z(\boldsymbol{\rho}'_{ij})w_{ij} \qquad (15)$$

where P is the number of quadrature points on each segment and w_{ij} is the weight of the quadrature rule on the jth point of the ith

segment. Choosing the quadrature points as the observation points and performing the point-matching procedure on these quadrature points results in the following algebraic matrix equation

$$E_z^i(\boldsymbol{\rho}_{mn}) = \sum_{i=1}^{N}\sum_{j=1}^{P} g(\boldsymbol{\rho}_{mn}, \boldsymbol{\rho}'_{ij}) J_z(\boldsymbol{\rho}'_{ij}) w_{ij} \tag{16}$$

where $m = 1, 2, \cdots, N$ and $n = 1, 2, \cdots, P$. This is a $NP \times NP$ matrix equation with NP unknown values of the current density on NP quadrature points. The resulting matrix equation is also solved using iteration methods when the matrix size is very large. The problem in this process is that the diagonal elements in the matrix cannot be determined because the observation points coincide the source points with the logarithm singularity of the Green's function. This problem can be solved by using a local correction based on the singularity treatment in [20]. Due to the complexity of the local correction with a high order, we adopt a simpler but efficient procedure proposed in [12] to evaluate the diagonal elements. We rewrite (16) by extracting the self term and obtain

$$E_z^i(\boldsymbol{\rho}_{mn}) = \sum_{i=1}^{N}\sum_{j=1}^{P} g(\boldsymbol{\rho}_{mn}, \boldsymbol{\rho}'_{ij}) J_z(\boldsymbol{\rho}'_{ij}) w_{ij} + A \tag{17}$$

where

$$A = \sum_{j=1}^{P} g(\boldsymbol{\rho}_{mn}, \boldsymbol{\rho}'_{mj}) J_z(\boldsymbol{\rho}'_{mj}) w_{mj} \tag{18}$$

is the self term. The self term can be further rewritten as

$$\begin{aligned} A &= \sum_{j=1}^{P} g(\boldsymbol{\rho}_{mn}, \boldsymbol{\rho}'_{mj}) J_z(\boldsymbol{\rho}'_{mj}) w_{mj} + g(\boldsymbol{\rho}_{mn}, \boldsymbol{\rho}'_{mn}) J_z(\boldsymbol{\rho}'_{mn}) w_{mn} \\ &= \sum_{j=1}^{P} [J_z(\boldsymbol{\rho}'_{mj}) - J_z(\boldsymbol{\rho}'_{mn})] g(\boldsymbol{\rho}_{mn}, \boldsymbol{\rho}'_{mj}) w_{mj} + J_z(\boldsymbol{\rho}'_{mn}) B \end{aligned} \tag{19}$$

where

$$B = \int_{\Delta C_m} g(\boldsymbol{\rho}_{mn}, \boldsymbol{\rho}') d\ell'. \tag{20}$$

The integral (20) can be evaluated in a closed-form by using the small argument approximation of the Hankel function [18], namely

$$B = \Delta C_m \left[1 - j\frac{2}{\pi} \ln\left(\frac{1.781\kappa\Delta C_m}{4e}\right)\right] \tag{21}$$

where $e = 2.718$. This integral can also be efficiently evaluated using the generalized quadrature rule proposed in [20].

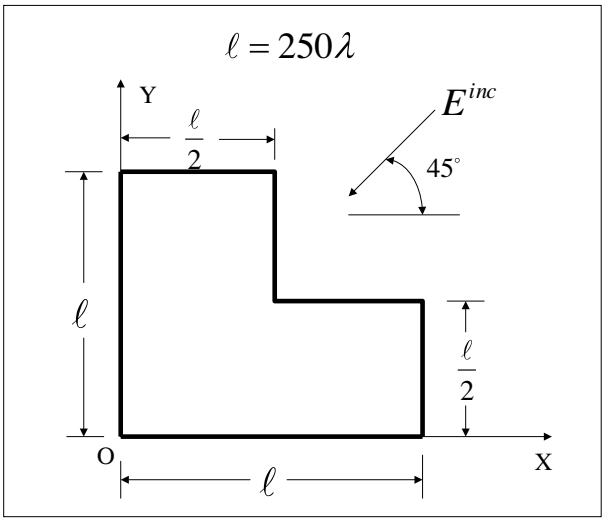

Figure 2. Geometry of a 2D conducting L-shape cylinder.

5. NUMERICAL EXAMPLES

Example 1: Scattering by a 2D conducting L-shaped cylinder. Consider a 2D conducting L-shaped scatterer as shown in Fig. 2. The scattering by this structure has been analyzed by several authors [21, 22], but the size was limited to be electrically small or medium. We select $\ell = 250\lambda$ here to enlarge the size of the scatterer with a circumference of 1000λ, where λ is the wavelength. Fig. 3 shows the corresponding numerical solution for the normalized current density on the contour of the scatterer in the TM case using the MoM with 20 unknowns per wavelength. The large numerical noise is clearly seen in this plot. In contrast, the MBMM solution, as shown in Fig. 4, with only 10 unknowns per wavelength is more attractive because only a very low numerical noise appears. The Nyström method solution is plotted in Fig. 5, but it cannot provide a better approximation for the current density if we discretize the contour of the scatterer into 5000 segments with 4 quadrature points at each.

Example 2: Scattering by a 2D conducting duct. This problem is taken from [23] and the geometry is plotted in Fig. 6. We choose $r = 64\lambda$, yielding a circumference of 1024λ. Figs. 7–9 show the corresponding MoM solutions for the normalized current density on the duct contour in the TM case with different discretizations. Fig. 10 sketches the MBMM solution for the current density with 10 unknowns

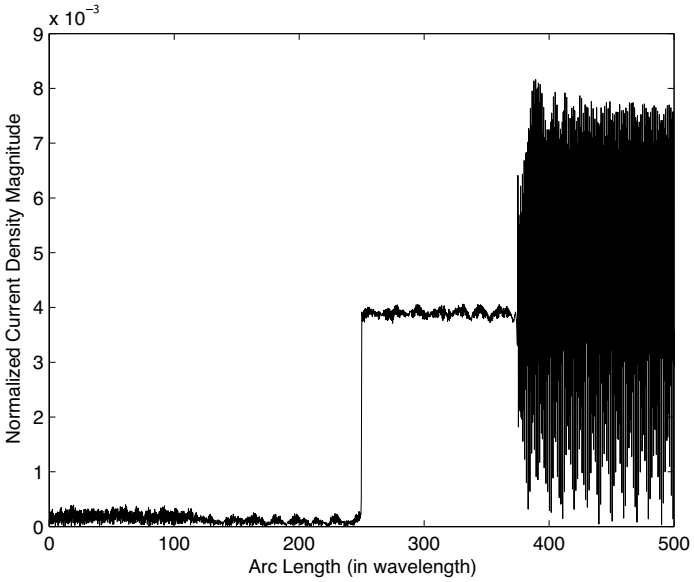

Figure 3. MoM solution with 20 unknowns per wavelength for the current on the L-shape cylinder.

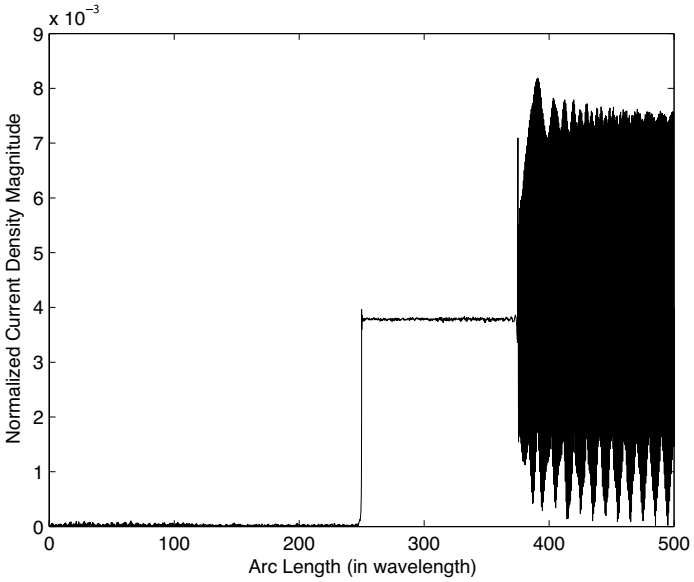

Figure 4. MBMM solution with 10 unknowns per wavelength for the current on the L-shape cylinder.

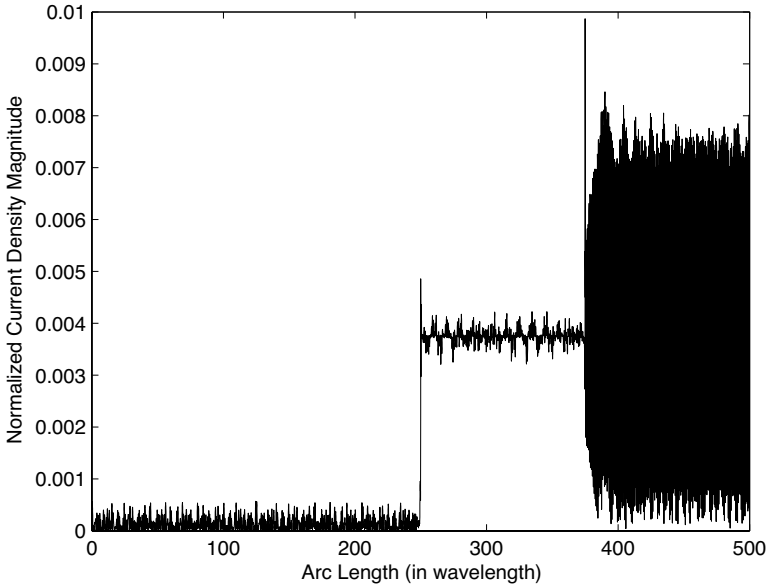

Figure 5. Nyström solution with 5000×4 unknowns for the current on the L-shape cylinder.

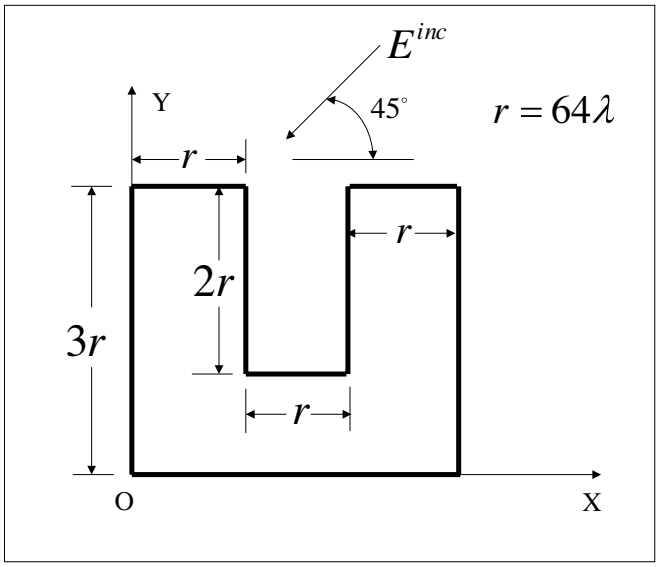

Figure 6. Geometry of a 2D conducting duct scatterer.

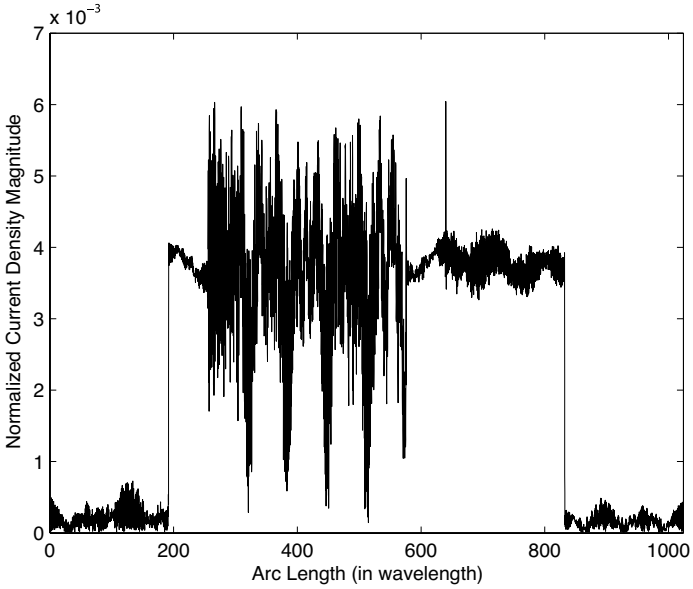

Figure 7. MoM solution with 10 unknowns per wavelength for the current on the duct scatterer.

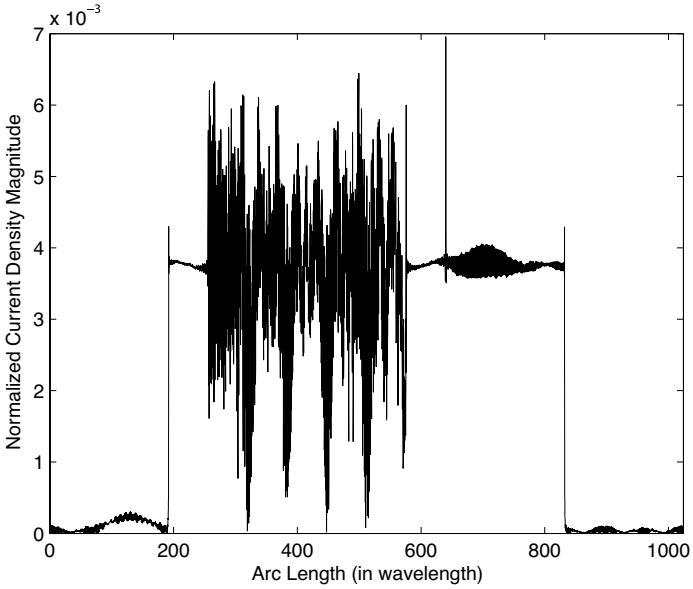

Figure 8. MoM solution with 20 unknowns per wavelength for the current on the duct scatterer.

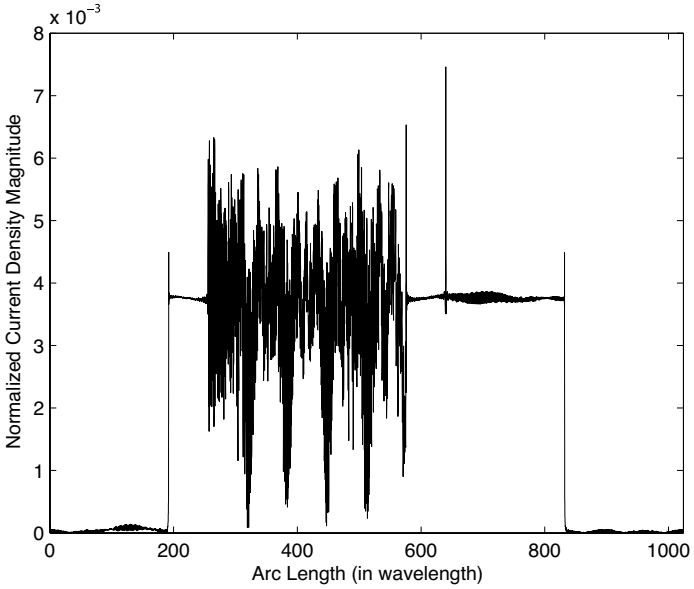

Figure 9. MoM solution with 30 unknowns per wavelength for the current on the duct scatterer.

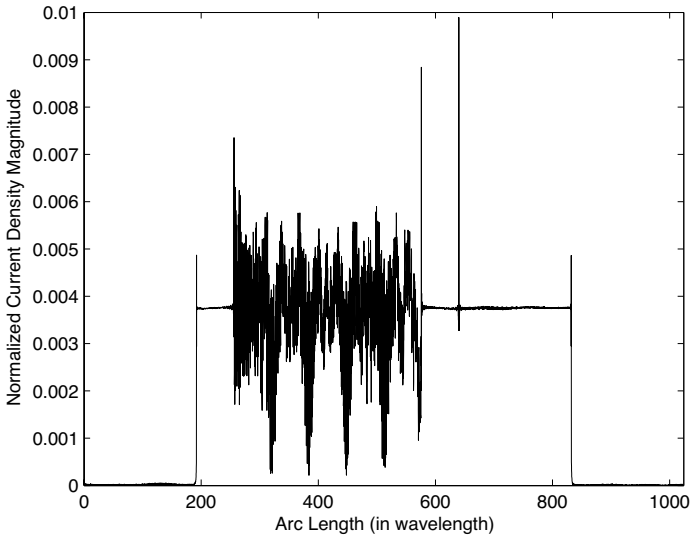

Figure 10. MBMM solution with 10 unknowns per wavelength for the current on the duct scatterer.

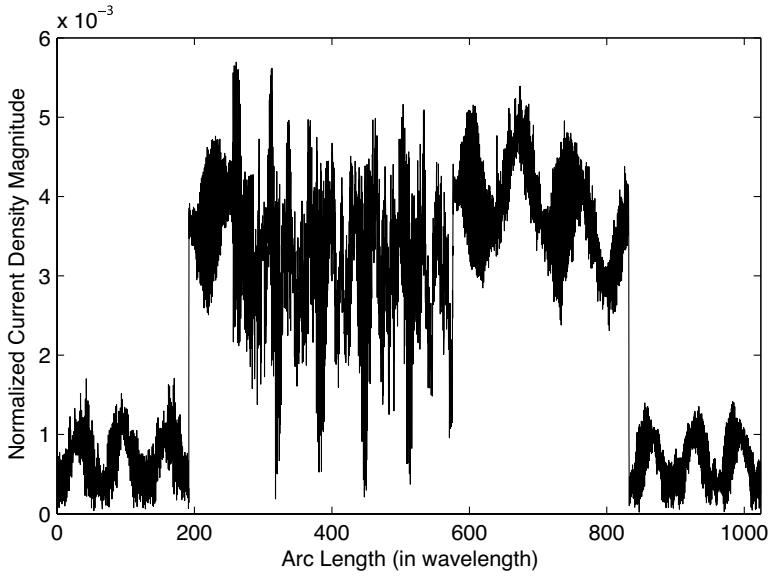

Figure 11. Nyström solution with 5000×4 unknowns for the current on the duct scatterer.

per wavelength. It is clear that the MBMM solution is better than the MoM solution with the finest mesh. The Nyström solution is also shown in the Fig. 11 and the solution is the worst due to the insufficient discretization or quadrature points.

6. CONCLUSION

The multiscalet based algorithm is used to solve for the scattering problems with a very large size reaching 1000λ and 1024λ. The numerical solutions are very stable due to the high-order representation of the basis functions and derivative tracking for the unknown functions. The discretization scheme with 10 unknowns per wavelength is unchanged compared with the electrically small problems. In the contrast, the lower-order MoM produces much more numerical noises in the numerical solutions and the finer discretization is required for a better approximation. The Nyström method is also implemented in the 2D scattering problems with a higher-order local correction for the singular elements in the system matrix. However, the numerical solutions are not better if the quadrature points are not enough. Choosing more quadrature points increases the resulting system matrix size sharply, leading to a cancellation of the advantages of the method.

Overall, the multiscalet based algorithm is the most robust. If its MoM matrix is incorporated with the FMM, a new fast hybrid algorithm for solving extremely large problems is possibly yielded.

REFERENCES

1. Harrington, R. F., *Field Computation by Moment Methods*, IEEE Press, New York, 1993.
2. Al Sharkawy, M. H., V. Demir, and A. Z. Elsherbeni, "The iterative multi-region algorithm using a hybrid finite difference frequency domain and method of moment techniques," *Progress In Electromagnetics Research*, PIER 57, 19–32, 2006.
3. Wang, S., X. Guan, D. Wang, X. Ma, and Y. Su, "Electromagnetic scattering by mixed conducting/dielectric objects using higher-order MOM," *Progress In Electromagnetics Research*, PIER 66, 51–63, 2006.
4. Chew, W. C., J. M. Jin, E. Michielssen, and J. M. Song, *Fast and Efficient Algorithms in Computational Electromagnetics*, Artech House, Boston, 2001.
5. Coifman, R., V. Rokhlin, and S. Wandzura, "The fast multipole method for the wave equation: A pedestrian prescription," *IEEE Ant. Propag. Mag.*, Vol. 35, No. 3, 7–12, 1993.
6. Song, J. M. and W. C. Chew, "Multilevel fast-multipole algorithm for solving combined field integral equations of electromagnetic scattering," *Micro. Opt. Tech. Lett.*, Vol. 10, No. 1, 14–19, 1995.
7. Song, J. M. and W. C. Chew, "Large scale computations using FISC," *IEEE Antennas Propag. Soc. Int. Symp.*, Salt Lake City, Utah, Vol. 4, 1856–1859, 2000.
8. Pan, X. M. and X. Q. Sheng, "A highly efficient parallel approach of multi-level fast multipole algorithm," *Journal of Electromagnetic Waves and Applications*, Vol. 20, No. 8, 1081–1092, 2006.
9. Bucci, O. M., G. D'Elia, and M. Santojanni, "A fast multipole approach to 2D scattering evaluation based on a non redundant implementation of the method of auxiliary sources," *Journal of Electromagnetic Waves and Applications*, Vol. 20, No. 13, 1715–1723, 2006.
10. Canino, L. S., J. J. Ottusch, M. A. Stalzer, J. L. Visher, and S. Wandzura, "Numerical solution of the Helmholtz equation in 2D and 3D using a high-order Nyström discretization," *J. Comput. Phys.*, Vol. 146, No. 2, 627–663, 1998.

11. Gedney, S. D., "On deriving a locally corrected Nyström scheme from a quadrature sampled moment method," *IEEE Trans. Antennas Propagat.*, Vol. 51, No. 9, 2402–2412, 2003.
12. Burghignoli, P., C. Di Nallo, F. Frezza, and A. Galli, "A simple Nyström approach for the analysis of 3D arbitrarily shaped conducting and dielectric bodies," *Int. J. Numer. Model. El.*, Vol. 16, No. 2, 179–194, 2003.
13. Pan, G., *Wavelets in Electromagnetics and Device Modeling*, John Wiley & Sons, Hoboken, 2003.
14. Pan, G., M. Tong, and B. Gilbert, "Multiwavelet based moment method under discrete Sobolev-type norm," *Micro. Opt. Tech. Lett.*, Vol. 40, No. 1, 47–50, 2004.
15. Tong, M., G. Pan, and G. Lei, "Full-wave analysis of coupled lossy transmission lines using multiwavelet-based method of moments," *IEEE Trans. Microw. Theory Tech.*, Vol. 53, No. 7, 2362–2370, 2005.
16. Zunoubi, M. R. and A. A. Kishk, "A combined Bi-Cgstab (1) and wavelet transform method for EM problems using method of moments," *Progress In Electromagnetics Research*, PIER 52, 205–224, 2005.
17. Alyt, O. M., A. S. Omar, and A. Z. Elsherbeni, "Detection and localization of RF radar pulses in noise environments using wavelet packet transform and higher order statistics," *Progress In Electromagnetics Research*, PIER 58, 301–317, 2006.
18. Balanis, C. A., *Advanced Engineering Electromagnetics*, John Wiley & Sons, New York, 1989.
19. Adams, L. and J. L. Nazareth, *Linear and Nonlinear Conjugate Gradient-related Methods*, Society for Industrial and Applied Mathematics, Philadelphia, 1996.
20. Kolm, P. and V. Rokhlin, "Numerical quadratures for singular and hypersingular integrals," *Comput. Math. Appl.*, Vol. 41, No. 3, 327–352, 2001.
21. Wagner, R. L. and W. C. Chew, "A study of wavelets for the solution of electromagnetic integral equation," *IEEE Trans. Antennas Propagat.*, Vol. 43, No. 8, 802–810, 1995.
22. Pan, G., Y. V. Tretiakov, and B. Gilbert, "Smooth local cosine based Galerkin method for scattering problems," *IEEE Trans. Antennas Propagat.*, Vol. 51, No. 6, 1177–1184, 2003.
23. Deng, H. and H. Ling, "Fast solution of electromagnetic integral equations using adaptive wavelet packet transform," *IEEE Trans. Antennas Propagat.*, Vol. 47, No. 4, 674–682, 1999.

24. Press, W. H., S. A. Teukolsky, W. T. Vetterling, and B. P. Flannery, *Numerical Recipes in FORTRAN: the art of scientific computing*, 2nd edition, Cambridge University Press, New York, 1992.
25. Abramowitz, M. and I. A. Stegun, *Handbook of Mathematical Functions with Formulas, Graphs and Mathematical Tables*, Dover, New York, 1970.